Progress In Electromagnetics Research M, Vol. 67, 55–64, 2018

DOA Estimation Using Triply Primed Arrays Based on Fourth-Order Statistics

Kai-Chieh Hsu and Jean-Fu Kiang*

Abstract—A triply primed array (TPA) is configured on three mutually primed integers (N_1, N_2 and N_3), which operates with $O(N_1N_2N_3)$ degree-of-freedoms to estimate the direction-of-arrivals (DOAs) of multiple incident quasi-stationary signals. The set of unique and contiguous lags of the proposed TPA is searched and verified. Simulation results verify that the proposed TPA can detect more incident signals with higher accuracy than its compatible counterparts.

1. INTRODUCTION

Direction-of-arrival (DOA) estimation is critical to radars and wireless communication systems. By processing the received signals from an N-element uniform linear array (ULA), subspace-based algorithms such as multiple signal classification (MUSIC) [1] and estimation of signal parameters via rotational invariance techniques (ESPRIT) [2] can be used to estimate at most $N-1$ sources. A Khatri-Rao (KR) subspace-based algorithm was proposed to increase the degrees-of-freedom (DOF) of an N-element ULA to $2N-2$ [3].

Several array configurations with higher DOF have been proposed. In [4], a nested array was proposed to detect $O(N^2)$ sources with N sensors. However, the inter-element spacing is so small that mutual coupling effect becomes severe. In [5], a co-prime array was proposed, which is composed of two interleaved ULAs, one with M elements at N-interval spacing and the other with N elements at M-interval spacing, where M and N are mutually primed integers. The number of elements in one constituent array was increased from M to $2M$, extending the range of contiguous virtual lags to $-MN \sim MN$ [6]. By applying MUSIC algorithm, with the covariance matrix processed by a spatial smoothing technique, the DOF reaches $O(MN)$. In [7], a MUSIC-based method with array interpolation and matrix denoising was proposed to fill the holes in a virtual coarray and reduce the estimation error of covariance matrix due to finite snapshots. In [8], an ESPRIT-based method was proposed to estimate the DOAs without resorting to spatial smoothing, peak search or a predefined grid.

Sparse signal processing techniques, such as compressive sensing (CS), have been used for DOA estimation. In [9], a CS-MUSIC algorithm was proposed on the relation between multiple measurement vectors and the estimated DOAs. In [10], an ℓ_1-optimization was proposed for sparse signal recovery, where ℓ_1 norm was imposed to ensure sparsity. In [11], co-prime arrays were generalized to include nested array [4] as a special case. In [12], a nearest grid DOA estimation method, supported by Rife algorithm, was proposed to detect DOAs that were off the grid. In [13], a low-complexity ℓ_1-normalization was proposed to merge same or conjugated lags. In general, the CS methods render higher DOF than MUSIC and perform better than the latter. However, the CS methods have difficulties in estimating off-grid DOAs and take heavier computational load.

In the aforementioned algorithms, received signals up to the second-order statistics were used. The performance is expected to improve if higher-order statistics can be used. In [14], MUSIC algorithm

Received 24 January 2018, Accepted 24 March 2018, Scheduled 5 April 2018
* Corresponding author: Jean-Fu Kiang (jfkiang@ntu.edu.tw).
The authors are with the Department of Electrical Engineering, National Taiwan University, Taipei 106, Taiwan.

was applied to process fourth-order cumulant matrix to mitigate mutual coupling effects. In [15], ℓ_1-normalization was applied to a fourth-order difference matrix to increase the range of contiguous lags. In this work, we propose a triply primed array (TPA), which is composed of three arrays specified by three mutually primed integers. By processing fourth-order statistics, higher DOF can be acquired by increasing the numbers of lags and contiguous lags. This paper is organized as follows. The signal model is presented in Section 2, the properties of TPA are analyzed in Section 3, the DOA estimation algorithms and dimension-reduction approach are presented in Section 4, and the simulation results are discussed in Section 5. Finally, some conclusions are drawn in Section 6.

2. SIGNAL MODEL OF TRIPY PRIMED ARRAY

Figure 1 shows the proposed TPA, which is composed of three ULAs, with N_1, N_2 and N_3 sensors, respectively; where N_1, N_2 and N_3 are mutually primed integers. Without loss of generality, assume $N_1 < N_2 < N_3$ and the unit spacing is $d = \lambda/2$. The spacings in the first, second and third ULAs are N_2N_3d, N_1N_3d and N_1N_2d, respectively. The first sensors of the three ULAs are aligned at the origin, leading to a total of $N = N_1 + N_2 + N_3 - 2$ sensors in the TPA. The locations of the physical sensors in these three ULAs are specified in Γ_1, Γ_2 and Γ_3, respectively, with

$$\begin{aligned} &\Gamma_1 = \{n_1N_2N_3d \mid 0 \le n_1 \le N_1 - 1\}, \quad \Gamma_2 = \{n_2N_1N_3d \mid 0 \le n_2 \le N_2 - 1\}, \\ &\Gamma_3 = \{n_3N_1N_2d \mid 0 \le n_3 \le N_3 - 1\} \end{aligned} \tag{1}$$

Assume that there are M uncorrelated source signals. The DOA of the mth source signal s_m is θ_m, with $1 \le m \le M$. The signals received at the ℓth time interval can be represented as

$$\bar{x}_1[\ell] = \bar{\bar{A}}_1 \cdot \bar{s}[\ell] + \bar{n}_1[\ell], \quad \bar{x}_2[\ell] = \bar{\bar{A}}_2 \cdot \bar{s}[\ell] + \bar{n}_2[\ell], \quad \bar{x}_3[\ell] = \bar{\bar{A}}_3 \cdot \bar{s}[\ell] + \bar{n}_3[\ell] \tag{2}$$

where $\bar{s}[\ell]$ is the source signal vector, and $\bar{\bar{A}}_\alpha$ and $\bar{n}_\alpha$ are the steering matrix and noise vector, respectively, of the αth ULA, with $\alpha = 1, 2, 3$. The mth column of each steering matrix is the steering vector associated with the mth source signal. Explicitly,

$$\begin{aligned} \bar{a}_1(\theta_m) &= \left[1, e^{jkN_2N_3d\sin\theta_m}, \ldots, e^{jkN_2N_3(N_1-1)d\sin\theta_m}\right]^t, \\ \bar{a}_2(\theta_m) &= \left[1, e^{jkN_1N_3d\sin\theta_m}, \ldots, e^{jkN_1N_3(N_2-1)d\sin\theta_m}\right]^t, \\ \bar{a}_3(\theta_m) &= \left[1, e^{jkN_1N_2d\sin\theta_m}, \ldots, e^{jkN_1N_2(N_3-1)d\sin\theta_m}\right]^t \end{aligned}$$

where $k = 2\pi/\lambda$ is the wavenumber. The additive white Gaussian noise vectors $\bar{n}_1[\ell]$, $\bar{n}_2[\ell]$ and $\bar{n}_3[\ell]$ have zero mean and covariance matrices $\sigma_n^2\bar{\bar{I}}_{N_1}$, $\sigma_n^2\bar{\bar{I}}_{N_2}$ and $\sigma_n^2\bar{\bar{I}}_{N_3}$ respectively, where $\bar{\bar{I}}_N$ is an $N \times N$

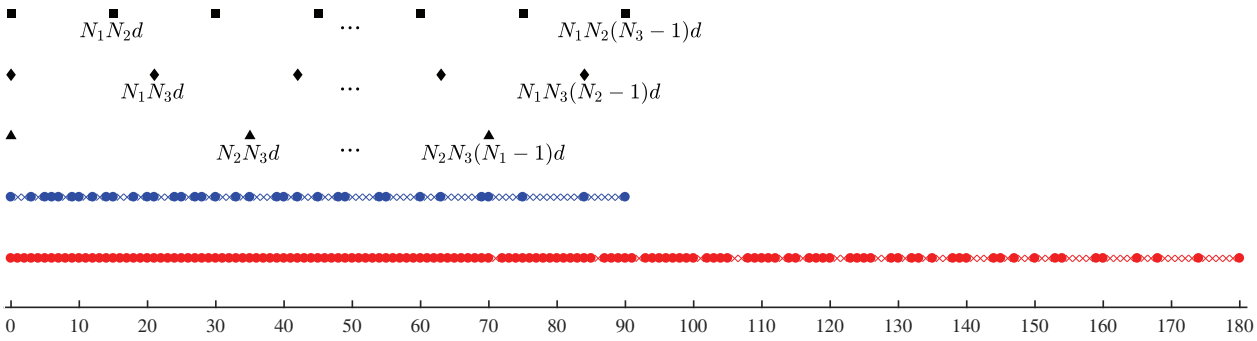

Figure 1. Configuration of proposed TPA, constituent physical subarrays and positive lags of second-order and fourth-order virtual arrays. ■: physical subarray at spacing N_1N_2d, ♦: physical subarray at spacing N_1N_3d, ▲: physical subarray at spacing N_2N_3d; ●: second-order virtual array, ×: second-order holes, ●: fourth-order virtual array, ×: fourth-order holes.

identity matrix. Each noise vector is assumed to be uncorrelated to the source signals and the other noise vectors. The received signals in (2) are concatenated as

$$\bar{x}[\ell] = \bar{\bar{A}} \cdot \bar{s}[\ell] + \bar{n}[\ell] \tag{3}$$

where

$$\bar{x}[\ell] = \begin{bmatrix} \bar{x}_1[\ell] \\ \bar{x}_2[\ell] \\ \bar{x}_3[\ell] \end{bmatrix}, \quad \bar{\bar{A}} = \begin{bmatrix} \bar{\bar{A}}_1 \\ \bar{\bar{A}}_2 \\ \bar{\bar{A}}_3 \end{bmatrix}, \quad \bar{n}[\ell] = \begin{bmatrix} \bar{n}_1[\ell] \\ \bar{n}_2[\ell] \\ \bar{n}_3[\ell] \end{bmatrix}$$

Assume that the source signals are wide-sense quasi-stationary and are measured over Q non-overlapped time frames, with each time frame containing L time intervals [3, 13]. The power of the mth source signal in the qth time frame can be represented as

$$P_{qm} = \mathrm{E}\left\{|s_m[\ell]|^2\right\}, \quad 1 \le q \le Q, (q-1)L \le \ell \le qL-1 \tag{4}$$

where P_{qm} with $1 \le q \le Q$ are wide-sense stationary and uncorrelated from each other, namely,

$$\mathrm{E}_q\{P_{qm}\} = \mu_m, \quad \mathrm{E}_q\left\{(P_{qm}-\mu_m)^2\right\} = \tilde{\sigma}_m^2 \tag{5}$$

The covariance matrix of the received signals in the qth time frame can be represented as

$$\bar{\bar{R}}_{xxq} = \mathrm{E}\{\bar{x}^q[\ell]\bar{x}^{q\dagger}[\ell]\} = \bar{\bar{A}} \cdot \bar{\bar{D}}_{xxq} \cdot \bar{\bar{A}}^\dagger + \sigma_n^2 \bar{\bar{I}}_N \tag{6}$$

where $\bar{x}^q[\ell]$ is the received signal at the qth time frame and $\bar{\bar{D}}_{xxq} = \mathrm{diag}\{P_{q1}, P_{q2}, \ldots, P_{qM}\}$. In practice, $\bar{\bar{R}}_{xxq}$ is estimated as

$$\hat{\bar{\bar{R}}}_{xxq} = \frac{1}{L} \sum_{\ell=(q-1)L}^{qL-1} \bar{x}^q[\ell]\bar{x}^{q\dagger}[\ell] \tag{7}$$

All the columns of $\bar{\bar{R}}_{xxq}$ are concatenated into an $N^2 \times 1$ vector as

$$\bar{y}_q = \mathrm{vec}\left\{\bar{\bar{R}}_{xxq}\right\} = \bar{\bar{B}} \cdot \bar{P}_q + \sigma_n^2 \bar{\nu}_N \tag{8}$$

where $\bar{P}_q = [P_{q1}, P_{q2}, \ldots, P_{qM}]^t$, $\bar{\nu}_N = \mathrm{vec}\{\bar{\bar{I}}_N\}$, and $\bar{\bar{B}} = \bar{\bar{A}}^* \odot \bar{\bar{A}}$ is the second-order difference manifold matrix, with $\odot$ the column-wise Kronecker product.

To obtain the fourth-order difference coarray, first take the expectation value of $\bar{y}_q$ to have

$$\bar{y}'_q = \mathrm{E}\{\bar{y}_q\} = \bar{\bar{B}} \cdot \bar{P}'_q + \sigma_n^2 \bar{\nu}_N \tag{9}$$

where $\bar{P}'_q = \mathrm{E}_q\left\{\bar{P}_q\right\} = [\mu_1, \mu_2, \ldots, \mu_M]^t$ Next, subtract (9) from (8) to obtain

$$\bar{y}''_q = \bar{y}_q - \bar{y}'_q = \bar{\bar{B}} \cdot \left(\bar{P}_q - \bar{P}'_q\right) = \bar{\bar{B}} \cdot \bar{P}''_q \tag{10}$$

Thus, Q signals are derived from the second-order statistics of the original received signals.

Similar to (6) and (7), derive the covariance matrix of $\bar{y}''_q$ and its estimation as

$$\bar{\bar{R}}_{yy} = \mathrm{E}\{\bar{y}''_q \bar{y}''^\dagger_q\} = \bar{\bar{B}} \cdot \bar{\bar{D}}_{yy} \cdot \bar{\bar{B}}^\dagger \tag{11}$$

$$\hat{\bar{\bar{R}}}_{yy} = \frac{1}{Q} \sum_{q=1}^{Q} \bar{y}''_q \bar{y}''^\dagger_q \tag{12}$$

where $\bar{\bar{D}}_{yy} = \mathrm{diag}\left\{\tilde{\sigma}_1^2, \tilde{\sigma}_2^2, \ldots, \tilde{\sigma}_M^2\right\}$. By vectorizing $\bar{\bar{R}}_{yy}$, we obtain

$$\bar{z} = \mathrm{vec}\left\{\bar{\bar{R}}_{yy}\right\} = \bar{\bar{C}} \cdot \bar{\psi} \tag{13}$$

where $\bar{\psi} = \left[\tilde{\sigma}_1^2, \tilde{\sigma}_2^2, \ldots, \tilde{\sigma}_M^2\right]^t$ and $\bar{\bar{C}} = \bar{\bar{B}}^* \odot \bar{\bar{B}}$ is the fourth-order difference manifold matrix.

3. PROPERTIES OF TRIPLY PRIMED ARRAY

3.1. Second-Order Virtual Array

Define self-difference matrices and cross-difference matrices between these three constituent subarrays as

$$\begin{aligned}\bar{\bar{R}}_{\alpha\alpha q} &= \mathrm{E}\{\bar{x}_\alpha^q[\ell]\bar{x}_\alpha^{q\dagger}[\ell]\} = \bar{\bar{A}}_\alpha \cdot \bar{\bar{D}}_{xxq} \cdot \bar{\bar{A}}_\alpha^\dagger + \sigma_\alpha^2 \bar{\bar{I}}_{N_\alpha} \\ \bar{\bar{R}}_{\alpha\beta q} &= \mathrm{E}\{\bar{x}_\alpha^q[\ell]\bar{x}_\beta^{q\dagger}[\ell]\} = \bar{\bar{A}}_\alpha \cdot \bar{\bar{D}}_{xxq} \cdot \bar{\bar{A}}_\beta^\dagger + \sigma_\beta^2 \bar{\bar{W}}_{\alpha\beta}\end{aligned} \tag{14}$$

where $1 \le \alpha, \beta \le 3$, $\bar{\bar{W}}_{\alpha\beta}$ is an $N_\alpha \times N_\beta$ matrix with the 00th entry equal to 1 and the other entries equal to zero. The uvth entry of $\bar{\bar{R}}_{12q}$ is

$$R_{12q}[u,v] = \begin{cases} \displaystyle\sum_{m=1}^{M} P_{qm} e^{jkN_3(uN_2 - vN_1)d\sin\theta_m} + \sigma_n^2, \\ \qquad u = v = 0 \\ \displaystyle\sum_{m=1}^{M} P_{qm} e^{jkN_3(uN_2 - vN_1)d\sin\theta_m}, \\ \qquad u \neq 0 \text{ or } v \neq 0 \end{cases} \tag{15}$$

It is observed that $R_{12q}[u,v]$ and $R_{12q}[N_1 - u, N_2 - v]$ are conjugate to each other with $u, v \neq 0$. In addition, the lags of entries in the first column of $\bar{\bar{R}}_{21q}$ overlap with those of some diagonal entries of $\bar{\bar{R}}_{11q}$, and the lags of entries in the first row of $\bar{\bar{R}}_{21q}$ overlap with those in some diagonal entries of $\bar{\bar{R}}_{22q}$, which implies that $\bar{\bar{R}}_{21q}$ is redundant in counting the number of unique lags. As a result, only $\bar{\bar{R}}_{12q}$, $\bar{\bar{R}}_{23q}$ and $\bar{\bar{R}}_{31q}$ are needed. Thus, all the unique lags of a second-order virtual array are included in the union of $\Gamma_0 = \{0\}$ and six disjoint sets,

$$\begin{aligned}\Gamma_{12} &= \{N_3(n_1N_2 - n_2N_1)d \mid 1 \le n_1 \le N_1 - 1, 1 \le n_2 \le N_2 - 1\}, \\ \Gamma_{23} &= \{N_1(n_2N_3 - n_3N_2)d \mid 1 \le n_2 \le N_2 - 1, 1 \le n_3 \le N_3 - 1\}, \\ \Gamma_{31} &= \{N_2(n_3N_1 - n_1N_3)d \mid 1 \le n_1 \le N_1 - 1, 1 \le n_3 \le N_3 - 1\}, \\ \Gamma_{11} &= \{n_1N_2N_3d \mid 1 \le |n_1| \le N_1 - 1\}, \quad \Gamma_{22} = \{n_2N_1N_3d \mid 1 \le |n_2| \le N_2 - 1\}, \\ \Gamma_{33} &= \{n_3N_1N_2d \mid 1 \le |n_3| \le N_3 - 1\},\end{aligned} \tag{16}$$

where $\Gamma_{\alpha\beta} = \{p - q \mid p \in \Gamma_\alpha, q \in \Gamma_\beta, p, q \neq 0\}$.

3.2. Fourth-Order Virtual Array

Based on the six sets in Eq. (16), 36 fourth-order difference sets can be derived. Since all the second-order difference sets are symmetric, the derived fourth-order difference sets are also symmetric, and $\Gamma_{\alpha\beta,\alpha'\beta'} = \Gamma_{\alpha'\beta',\alpha\beta}$.

The difference lags between Γ_{11}, Γ_{22}, Γ_{33} and Γ_{12} are listed below.

$$\begin{aligned}\Gamma_{11,11} &= \{n_1N_2N_3d \mid 1 \le |n_1| \le 2N_1 - 2\}, \quad \Gamma_{22,22} = \{n_2N_1N_3d \mid 1 \le |n_2| \le 2N_2 - 2\}, \\ \Gamma_{33,33} &= \{n_3N_1N_2d \mid 1 \le |n_3| \le 2N_3 - 2\}, \\ \Gamma_{12,12} &= \{N_3(n_1N_2 - n_2N_1)d \mid 2 - N_1 \le n_1 \le N_1 - 2, 2 - N_2 \le n_2 \le N_2 - 2\}, \\ \Gamma_{12,11} &= \{N_3(n_1N_2 - n_2N_1)d \mid 2 - N_1 \le n_1 \le 2N_1 - 2, 1 \le n_2 \le N_2 - 1\}, \\ \Gamma_{12,22} &= \{N_3(n_1N_2 - n_2N_1)d \mid 1 \le n_1 \le N_1 - 1, 2 - N_2 \le n_2 \le 2N_2 - 2\}, \\ \Gamma_{12,33} &= \{(n_1N_2N_3 - n_2N_1N_3 - n_3N_1N_2)d \mid 1 \le n_1 \le N_1 - 1, 1 \le n_2 \le N_2 - 1, 1 \le |n_3| \le N_3 - 1\}, \\ \Gamma_{11,22} &= \{N_3(n_1N_2 - n_2N_1)d \mid 1 \le |n_1| \le N_1 - 1, 1 \le |n_2| \le N_2 - 1\}, \\ \Gamma_{22,33} &= \{N_1(n_2N_3 - n_3N_2)d \mid 1 \le |n_2| \le N_2 - 1, 1 \le |n_3| \le N_3 - 1\}, \\ \Gamma_{33,11} &= \{N_2(n_3N_1 - n_1N_3)d \mid 1 \le |n_1| \le N_1 - 1, 1 \le |n_3| \le N_3 - 1\},\end{aligned} \tag{17}$$

It is observed that $\Gamma_{12,12} \subseteq \Gamma_{11,22}$.

Let $\mu = N_3(n_1N_2 - n_2N_1)d \in \Gamma_{12,11}$, $\nu = N_3(n_1'N_2 - n_2'N_1)d \in \Gamma_{11,22}$ and $\xi = n_2''N_1N_3d \in \Gamma_{22,22}$. It is observed that

$$\begin{cases} \mu = \nu,\ (n_1', n_2') = (n_1, n_2), & 2 - N_1 \leq n_1 \leq N_1 - 1 \\ \mu = \nu,\ (n_1', n_2') = (n_1 - N_1, n_2 - N_2), & N_1 + 1 \leq n_1 \leq 2N_1 - 2 \\ \mu = \xi,\ n_2'' = N_2 - n_2, & n_1 = N_1 \end{cases} \tag{18}$$

which implies that $\Gamma_{12,11} \subseteq (\Gamma_{11,22} \cup \Gamma_{22,22})$. Similarly, $\Gamma_{12,22}$ is included in the union of some other sets. As a result, the remaining 7 sets in Eq. (17) are disjoint to one another.

Next, let $\mu = (n_2N_1N_3 - n_3N_1N_2 - n_1N_2N_3)d \in \Gamma_{23,11}$ and $\nu = (n_1'N_2N_3 - n_2'N_1N_3 - n_3'N_1N_2)d \in \Gamma_{12,33}$. It is observed that

$$(n_1', n_2', n_3') = \begin{cases} (N_1 - n_1, N_2 - n_2, n_3), & n_1 \leq 0 \\ (-n_1, N_2 - n_2, -N_3 + n_3), & n_1 > 0 \end{cases} \tag{19}$$

which implies that $\Gamma_{23,11} = \Gamma_{12,33}$. Let $\mu = (n_1N_2N_3 - n_2N_1N_3 + n_3N_1N_2)d \in \Gamma_{12,23}$, $\nu = (n_1'N_2N_3 - n_2'N_1N_3 - n_3'N_1N_2)d \in \Gamma_{12,33}$ and $\xi = (n_3''N_1N_2 - n_1''N_2N_3)d \in \Gamma_{33,11}$. It is observed that

$$\begin{cases} \mu = \nu,\ (n_1', n_2', n_3') = (n_1, n_2, -n_3), & 2 \leq n_2 \leq N_2 - 1 \\ \mu = \nu,\ (n_1', n_2', n_3') = (n_1, n_2 - N_2, -n_3 + N_3), & N_2 + 1 \leq n_2 \leq 2N_2 - 2 \\ \mu = \xi,\ (n_1'', n_3'') = (-n_1, n_3 - N_3), & n_2 = N_2 \end{cases} \tag{20}$$

which implies that the lags in $\Gamma_{12,23}$ are included in $\Gamma_{12,33}$ or $\Gamma_{33,11}$. From Eqs. (18)–(20), all the fourth-order difference lags are included in 8 disjoint sets, $\Gamma_{11,11}$, $\Gamma_{22,22}$, $\Gamma_{33,33}$, $\Gamma_{11,22}$, $\Gamma_{22,33}$, $\Gamma_{33,11}$, $\Gamma_{12,33}$ and Γ_0. The number of unique fourth-order difference lags will be equal to the sum of cardinality of these 8 sets.

It is observed that the lags in $\Gamma_{11,11}$, $\Gamma_{22,22}$, $\Gamma_{33,33}$ and $\Gamma_{12,33}$ are mutually disjoint. On the other hand, some lags in $\Gamma_{11,22}$, $\Gamma_{22,33}$ and $\Gamma_{33,11}$ are overlapped. Consider $\mu = N_3(n_1N_2 - n_2N_1)d \in \Gamma_{11,22}$ and $\nu = N_3(n_1'N_2 - n_2'N_1)d \in \Gamma_{11,22}$, $\mu = \nu$ only when $(n_1', n_2') = (n_1 - N_1, n_2 - N_2)$ and $n_1, n_2 > 0$, leading to $2(N_1 - 1)2(N_2 - 1) - (N_1 - 1)(N_2 - 1) = 3(N_1 - 1)(N_2 - 1)$ unique lags in $\Gamma_{11,22}$. As a result, the number of unique lags in the fourth-order difference set is

$$\begin{aligned} \tau_u &= (4N_1 - 4) + (4N_2 - 4) + (4N_3 - 4) + 3(N_1 - 1)(N_2 - 1) + 3(N_2 - 1)(N_3 - 1) \\ &\quad + 3(N_1 - 1)(N_3 - 1) + 2(N_1 - 1)(N_2 - 1)(N_3 - 1) + 1 \\ &= 2N_1N_2N_3 + N_1N_2 + N_2N_3 + N_3N_1 - 8 \end{aligned} \tag{21}$$

It is also observed that the contiguous lags in the fourth-order difference set fall in the range $[-\tau_c, \tau_c]$, with $\tau_c = N_1N_2 + N_2N_3 + N_3N_1 - 1$. Note that lag at $N_1N_2 + N_2N_3 + N_3N_1$ does not belong to any of the 8 sets defined in Section III-B.

4. DOA ESTIMATION ALGORITHMS

Conventional subspace-based algorithms like MUSIC and ESPRIT require the rank of covariance matrix be higher than the number of source signals. As shown in Eq. (13), $\bar{\psi}$ is a vector, and the covariance matrix $\bar{\bar{R}}_{zz} = \bar{z}\bar{z}^{\dagger}$ is of rank one. A spatial-smoothing MUSIC (SS-MUSIC) algorithm can be applied to a virtual array based on $\bar{z}$, with rank significantly higher than one. A CS approach can be applied to solve an ℓ_1 optimization problem instead, with no restriction to the rank. These two methods are briefly reviewed in this Section.

4.1. Spatial-smoothing MUSIC Algorithm

The SS-MUSIC algorithm was proposed to increase the rank [6], but it can only be applied to virtual arrays with contiguous lags. To apply SS-MUSIC, non-contiguous lags of $\bar{z}$ are first removed to form

$$\bar{z}_c = \bar{\bar{C}}_c \cdot \bar{\psi} = [z_c[-\tau_c], z_c[-\tau_c + 1], \ldots, z_c[\tau_c - 1], z_c[\tau_c]]^t \tag{22}$$

where $\bar{\bar{C}}_c$ is constructed on a ULA with $2\tau_c+1$ sensors located from $-\tau_c d$ to $\tau_c d$. Next, construct τ_c+1 sub-vectors, each with τ_c+1 elements, as

$$\bar{z}_{c\xi} = [z_c[\xi-\tau_c], z_c[\xi-\tau_c+1], \ldots, z_c[\xi-1], z_c[\xi]]^t, \quad 0 \le \xi \le \tau_c \tag{23}$$

Then derive a matrix

$$\bar{\bar{R}}_{zz,ss} = \frac{1}{\tau_c+1}\sum_{\xi=0}^{\tau_c} \bar{z}_{c\xi}\bar{z}_{c\xi}^{\dagger} \tag{24}$$

of which the rank is τ_c+1. The MUSIC algorithm is then applied to $\bar{\bar{R}}_{zz,ss}$ to estimate the DOAs.

4.2. Compressive Sensing Algorithm

Before applying the CS approach, first formulate a sensing matrix $\bar{\bar{C}}_g$ composed of G steering vectors as

$$\bar{\bar{C}}_g = [\bar{c}_g(\phi_1), \bar{c}_g(\phi_2), \ldots, \bar{c}_g(\phi_G)] \tag{25}$$

where

$$\bar{c}_g(\phi_\alpha) = [\bar{a}^*(\phi_\alpha)\otimes\bar{a}(\phi_\alpha)]\otimes[\bar{a}^*(\phi_\alpha)\otimes\bar{a}(\phi_\alpha)]$$
$$\phi_\alpha = -90^\circ + 180^\circ(\alpha-1)/(G-1), \qquad 1 \le \alpha \le G$$

and $\otimes$ stands for Kronecker product. Then, Eq. (13) is transformed to an ℓ_1-norm minimization problem

$$\bar{\psi}_g^\circ = \arg\min_{\bar{\psi}_g} \|\bar{\psi}_g\|_1 \ \text{ s.t. } \ \|\bar{z} - \bar{\bar{C}}_g\cdot\bar{\psi}_g\|_2 < \epsilon \tag{26}$$

where ϵ is a given error bound, and $\|\cdot\|_p$ means the ℓ_p norm. Eq. (26) can be solved by using a software package CVX [16, 17]. The indices of nonzero entries in $\bar{\psi}_g^\circ$ are mapped to the estimated DOAs.

4.3. Dimension-Reduced Algorithm

The dimension of $\bar{\bar{C}}$ in Eq. (13) is $N^4\times G$, making the computational load impractical for real-time applications. In this Subsection, a modified version of dimension-reduced approach [13] for coprime arrays is proposed to support the TPA.

The expression in Eq. (15) indicates that some entries of $\bar{y}_q$ in Eq. (8) have the same lag or conjugated lag, which can be merged to reduce the dimension and increase the accuracy of DOA estimation. Entries with the same lags should have the same value in principle, but they are different in practice due to noise or other errors. Taking the average of different entries associated with a lag results in better accuracy of DOA estimation. To begin with, construct a vector

$$\bar{y}_{\alpha\alpha q} = [r_{\alpha\alpha q}^*[N_\alpha-1], \ldots, r_{\alpha\alpha q}^*[1], r_{\alpha\alpha q}[1], \ldots, r_{\alpha\alpha q}[N_\alpha-1]]^t, \qquad \alpha = 1,2,3$$

with

$$r_{\alpha\alpha q}[n] = \frac{1}{2(N_\alpha-n)}\sum_{n'=0}^{N_\alpha-1-n}\left(R_{\alpha\alpha q}[n+n',n'] + R_{\alpha\alpha q}^*[n',n+n']\right) \tag{27}$$

Then, vectorize $\bar{\bar{R}}'_{12q}$ to obtain $\bar{y}_{12q}$, with the uvth entry of $\bar{\bar{R}}'_{12q}$ defined as

$$R'_{12q}[u,v] = R_{12q}[u+1,v+1] + R_{12q}^*[N_1-1-u, N_2-v-1] \tag{28}$$

Similarly, $\bar{y}_{23q}$ and $\bar{y}_{31q}$ are obtained by vectorizing $\bar{\bar{R}}'_{23q}$ and $\bar{\bar{R}}'_{31q}$, respectively.

Next, form a dimension-reduced vector $\bar{y}_{qr}$ as

$$\bar{y}_{qr} = [y_{0q}, \bar{y}_{11q}^t, \bar{y}_{22q}^t, \bar{y}_{33q}^t, \bar{y}_{12q}^t, \bar{y}_{23q}^t, \bar{y}_{31q}^t]^t = \bar{\bar{B}}_{\Phi_B}\cdot\bar{\bar{P}}_q + \sigma_n^2\bar{w}, \tag{29}$$

where

$$y_{0q} = \frac{1}{N}\left(\sum_{n=0}^{N_1-1} R_{11q}[n,n] + \sum_{n=1}^{N_2-1} R_{22q}[n,n] + \sum_{n=1}^{N_3-1} R_{33q}[n,n]\right) \tag{30}$$

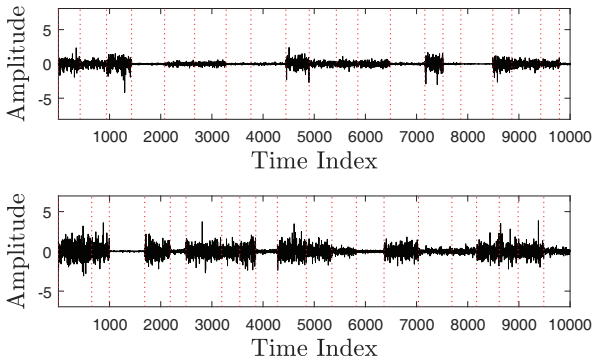

Figure 2. Simulated quasi-stationary signals (——), time frames are bounded by ....

$\bar{\bar{B}}_{\Phi_B}$ is a sub-matrix constituted of rows in $\bar{\bar{B}}$ which are indexed by Φ_B. Each element of Φ_B indicates a unique lag, and $\bar{w}$ is a vector with first entry equal to one and the others equal to zero. By applying the procedure in Eqs. (8)–(12) to $\bar{y}_{qr}$, we have

$$\bar{y}''_{qr} = \bar{y}_{qr} - \mathrm{E}\left\{\bar{y}_{qr}\right\} = \bar{\bar{B}}_{\Phi_B} \cdot \bar{\bar{P}}''_q$$

$$\bar{\bar{R}}_{yyr} = \mathrm{E}\{\bar{y}''_{qr}\bar{y}''^{\dagger}_{qr}\} = \bar{\bar{B}}_{\Phi_B} \cdot \bar{\bar{D}}_{yy} \cdot \bar{\bar{B}}^{\dagger}_{\Phi_B} \simeq \hat{\bar{\bar{R}}}_{yyr} = \frac{1}{Q}\sum_{q=1}^{Q} \bar{y}''_{qr}\bar{y}''^{\dagger}_{qr} \tag{31}$$

Then, Eq. (13) is modified as

$$\bar{z}' = \mathrm{vec}\left\{\bar{\bar{R}}_{yyr}\right\} = \bar{\bar{C}}' \cdot \bar{\psi} \tag{32}$$

where $\bar{\bar{C}}' = \bar{\bar{B}}^*_{\Phi_B} \odot \bar{\bar{B}}_{\Phi_B}$.

By imposing Eqs. (18)–(20), entries of $\bar{z}'$ with the same or conjugated lag are merged. A dictionary is prepared to record the corresponding lag of each entry in $\bar{z}'$. By using this dictionary, a dimension-reduced $\bar{z}_r$ is derived as

$$\bar{z}_r = \bar{z}_{\Phi_C} = \bar{\bar{C}}'_{\Phi_C} \cdot \bar{\psi} \tag{33}$$

where Φ_C is the set of indices corresponding to all the positive lags in the fourth-order difference set, and $|\Phi_C| = (\tau_u + 1)/2$. Finally, Eq. (26) is reformed as

$$\bar{\psi}^{\circ}_g = \arg\min_{\bar{\psi}_g} \|\bar{\psi}_g\|_1 \quad \text{s.t.} \quad \|\bar{z}_r - \bar{\bar{C}}'_{g,\Phi_C} \cdot \bar{\psi}_g\|_2 < \epsilon, \tag{34}$$

where $\bar{\bar{C}}'_g = \bar{\bar{B}}^*_{g,\Phi_B} \odot \bar{\bar{B}}^*_{g,\Phi_B}$.

5. SIMULATIONS AND DISCUSSIONS

In this work, TPA(3, 4, 5) and TPA(3, 5, 7) are constructed and compared with CPA(3, 5). TPA(3, 4, 5) and CPA(3, 5) are composed of 10 physical sensors, while TPA(3, 5, 7) is composed of 13 physical sensors. The unit spacing is $d = \lambda/2$ in all the three arrays. Without loss of generality, the DOAs of M signal sources are uniformly distributed over $[-60, 60°]$. Fig. 2 shows two sample segments of quasi-stationary source signals, with stationary intervals randomly chosen from a uniform distribution between [300, 700] samples [3]. The noise is specified in terms of the signal-to-noise ratio (SNR), which is defined as

$$\mathrm{SNR} = \frac{\frac{1}{T}\sum_{\ell=1}^{T} \mathrm{E}\left\{\left\|\bar{\bar{A}} \cdot \bar{s}[\ell]\right\|^2\right\}}{\mathrm{E}\left\{\|\bar{n}[\ell]\|^2\right\}} \tag{35}$$

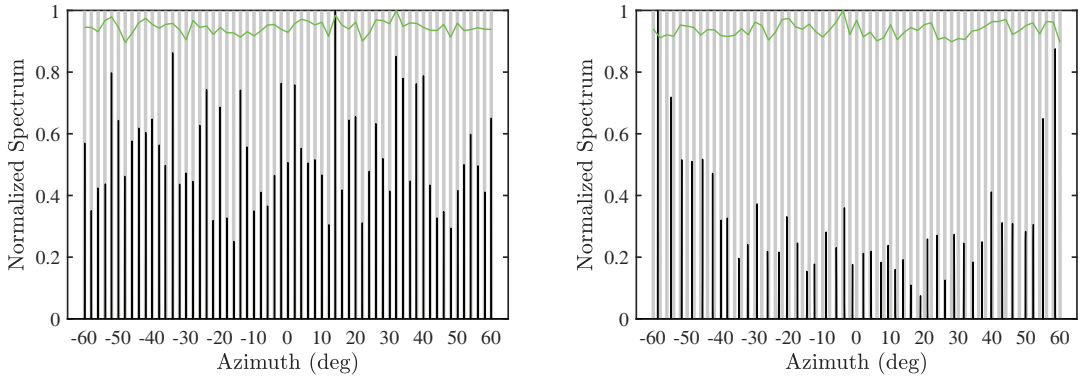

Figure 3. Normalized spectrum of (a) TPA (3, 4, 5) and (b) CPA (3, 5); $M = 61$, SNR $= 5\,\text{dB}$, $L = 500$, $Q = 1,000$. ———: estimated power spectrum; ——: actual power spectrum; ——: actual DOAs.

where $T = LQ$ [3]. The grid spacing of sensing matrix is 0.05°, and ϵ is chosen by trial-and-error. In each scenario, 100 Monte-Carlo realizations are simulated.

Figure 3 shows the normalized spectrum of TPA (3, 4, 5) and CPA (3, 5), respectively, where the actual power spectrum is $\bar{\psi}$ in Eq. (13), and the estimated power spectrum is ψ_g° in Eq. (34). The spectrum is normalized with respect to the largest entry in the original spectrum. The length of each time frame is fixed at L in the estimation algorithms. In Eq. (34), the vector length, $\|\bar{z}_r\|_2$, of TPA(3, 4, 5) and CPA(3, 5) is about 6, and the error bound is empirically chosen as $\epsilon = 1$. It is observed that all the signal sources are accurately detected by the TPA, but the CPA misses some signal sources and mistakenly detects non-existing signal sources between actual DOAs.

To compare the performance of different methods, a root-mean-square-error (RMSE) of DOA estimation is defined as

$$\text{RMSE} = \sqrt{\frac{1}{KM}\sum_{k=1}^{K}\sum_{m=1}^{M}|\tilde{\theta}_{km} - \theta_m|^2}, \tag{36}$$

where θ_m and $\tilde{\theta}_{km}$ are the actual DOA and the estimated DOA, respectively, of the mth source signal

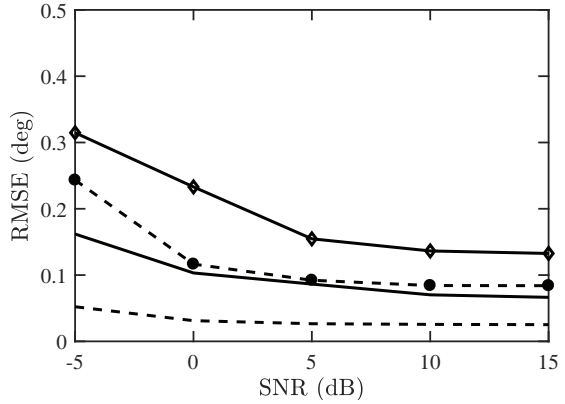

Figure 4. RMSE of DOA estimations under different SNRs; $M = 36$, $L = 500$, $Q = 1,000$. ——: TPA (3, 4, 5), CS; $-\bullet-$: TPA(3, 4, 5), SS-MUSIC; $-\diamond-$: CPA(3, 5), CS; $---$: TPA(3, 5, 7), CS.

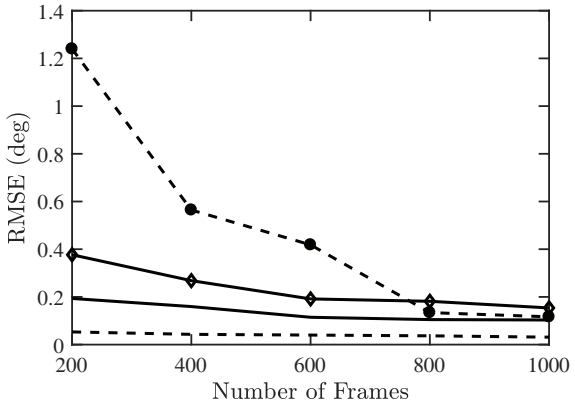

Figure 5. RMSE of DOA estimations with different numbers of frames; $M = 36$, $L = 500$, SNR $= 0\,\text{dB}$. ——: TPA (3, 4, 5), CS; $-\bullet-$: TPA (3, 4, 5), SS-MUSIC; $-\diamond-$: CPA (3, 5), CS; $---$: TPA (3, 5, 7), CS.

in the kth realization. Fig. 4 shows the RMSE of DOA estimation under different SNRs by using CS approach on TPA and CPA, as well as SS-MUSIC on TPA. In this case, the optimum values of ϵ for TPA (3, 4, 5), TPA(3, 5, 7) and CPA, under SNR $= [-5, 0, 5, 10, 15]$ dB, are $[4.3, 2, 1.5, 1, 1]$, $[4, 1, 0.8, 0.8, 0.8]$ and $[4, 1, 0.7, 0.6, 0.5]$, respectively. It is observed that the estimation results are less sensitive to the value of ϵ when SNR is greater than 0 dB. A larger ϵ is suggested when SNR is less than 0 dB. Fig. 4 shows the TPA supported by either SS-MUSIC or CS approach predicts accurate DOAs under all SNRs, especially when SNR < 0 dB. The CS approach predicts more accurate DOAs than the SS-MUSIC because the former makes use of all the unique lags, while the latter uses only contiguous lags.

Figure 5 shows the RMSE of DOA estimation with different numbers of frames. In this case, the optimum values of ϵ for TPA(3, 4, 5), TPA(3, 5, 7) and CPA, with $Q = [200, 400, 600, 800, 1000]$, are $[3.5, 3, 2, 2, 2]$, $[2, 2, 2, 2, 1]$ and $[1.5, 1, 1, 1, 1]$, respectively. The accuracy of DOA estimation is insensitive to ϵ when the latter is not far from the optimum value. The TPA supported by CS approach gives more accurate estimation than the other two, and the accuracy degrades smoothly when the number of frames decreases. The SS-MUSIC algorithm is more sensitive to the accuracy of $\hat{\bar{\bar{R}}}_{yy}$ in Eq. (12), as compared to the CS approach.

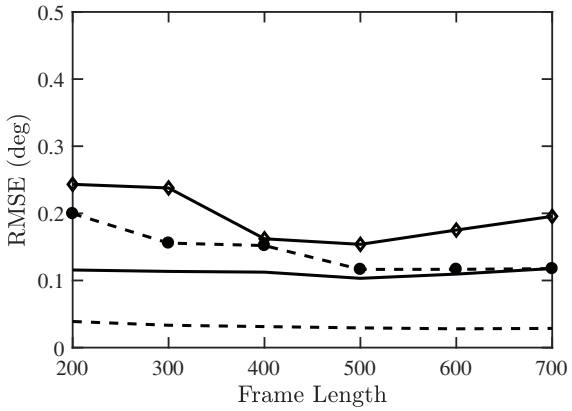

Figure 6. RMSE of DOA estimations with different lengths of frame; $M = 36$, $Q = 1,000$, SNR $= 0$ dB. ——: TPA (3, 4, 5), CS; $-\bullet-$: TPA (3, 4, 5), SS-MUSIC; $-\diamond-$: CPA (3, 5), CS; $---$: TPA (3 5, 7), CS.

Figure 6 shows the RMSE of DOA estimation with different lengths of frame. In this case, the optimum values of ϵ for TPA(3, 4, 5), TPA(3, 5, 7) and CPA, with $L = [200, 300, 400, 500, 600, 700]$, are $[3, 2.5, 2.5, 2, 2, 2]$, $[3, 2, 1.5, 1.2, 1, 1]$ and $[2.5, 2, 1, 1, 1, 1]$, respectively. Similar to the previous cases, the accuracy of DOA estimation is insensitive to ϵ if the latter is not far from the optimum value. It is observed that TPA supported by CS approach is hardly affected by the change of L due to the increased number of DOFs. The RMSE of CPA supported by CS approach and TPA supported by SS-MUSIC algorithm increases when L deviates from 500, possibly related to the estimation of power in each time frame.

In testing cases with known number of signal sources, optimum value of ϵ is tuned by trial-and-error under different SNR, numbers of frames or lengths of frame. The accuracy is slightly degraded when SNR > 0 dB if a fixed value of $\epsilon = 1$ is used. A rule of thumb is to choose a larger ϵ when the detection condition becomes worse, for example, low SNR, shorter length of frame or smaller number of frames. Otherwise, spurious peaks, sometimes stronger than actual peaks, may emerge in the spectrum. However, some DOAs may be missed if ϵ is chosen too large. A reasonable way is to choose $\epsilon = 1$ in the beginning and tune its magnitude according to SNR, number of time frames and frame length.

6. CONCLUSION

A triply primed array (TPA) based on three mutually prime numbers (N_1, N_2 and N_3) is proposed to achieve $O(N_1N_2N_3)$ DOFs in the fourth-order covariance matrices by exploiting the quasi-stationary signals. The properties of the proposed TPA are analyzed, and both SS-MUSIC algorithm and CS approach are applied to estimate the DOAs of signal sources. Simulation results show that the TPA can detect more signal sources with higher resolution than conventional CPA due to higher DOF of the former.

REFERENCES

1. Schmidt, R., "Multiple emitter location and signal parameter estimation," *IEEE Trans. Antennas Propagat.*, Vol. 34, No. 3, 276–280, 1986.
2. Roy, R. and T. Kailath, "ESPRIT-estimation of signal parameters via rotational invariance techniques," *IEEE Trans. Acous. Speech Signal Process.*, Vol. 37, No. 7, 984–995, 1989.
3. Mao, W. K., T. H. Hsieh, and C. Y. Chi, "DOA estimation of quasi-stationary signals with less sensors than sources and unknown spatial noise covariance: A Khatri-Rao subspace approach," *IEEE Trans. Signal Process.*, Vol. 58, No. 4, 2168–2180, 2010.
4. Pal, P. and P. P. Vaidyanathan, "Nested arrays: A novel approach to array processing with enhanced degrees of freedom," *IEEE Trans. Signal Process.*, Vol. 58, No. 8, 4167–4181, 2010.
5. Vaidyanathan, P. P. and P. Pal, "Sparse sensing with co-prime samplers and arrays," *IEEE Trans. Signal Process.*, Vol. 59, No. 2, 573–586, 2011.
6. Pal, P. and P. P. Vaidyanathan, "Coprime sampling and the MUSIC algorithm," *Proc. IEEE DSP/SPE Workshop*, 289–294, 2011.
7. Guo, M., T. Chen, and B. Wang, "An improved DOA estimation approach using coarray interpolation and matrix denoising," *Sensors*, Vol. 17, No. 5, 1140, 2017.
8. Zhou, C. and J. Zhou, "Direction-of-arrival estimation with coarray ESPRIT for coprime array," *Sensors*, Vol. 17, No. 8, 1779, 2017.
9. Kim, J. M., O. K. Lee, and J. C. Ye, "Compressive MUSIC: Revisiting the link between compressive sensing and array signal processing," *IEEE Trans. Info. Theory*, Vol. 58, No. 1, 278–301, 2012.
10. Zhang, Y. D., M. G. Amin, and B. Himed, "Sparsity-based DOA estimation using co-prime arrays," *IEEE Int. Conf. Acous. Speech Signal Process.*, 3967–3971, 2013.
11. Qin, S., Y. D. Zhang, and M. G. Amin, "Generalized coprime array configurations for direction-of-arrival estimation," *IEEE Trans. Signal Process.*, Vol. 63, No. 6, 1377–1390, 2015.
12. Xu, L., J. Chen, and Y. Gao, "Off-grid DOA estimation based on sparse representation and rife algorithm," *Prog. Electromag. Res. M*, Vol. 59, 193–201, 2017.
13. Shen, Q., W. Liu, W. Cui, S. Wu, Y. D. Zhang, and M. G. Amin, "Low-complexity direction-of-arrival estimation based on wideband co-prime arrays," *IEEE/ACM Trans. Audio Speech Lang. Process.*, Vol. 23, No. 9, 1445–1456, 2015.
14. Liu, S., J. Zhao, and Z. Xiao, "DOA estimation with sparse array under unknown mutual coupling," *Prog. Electromag. Res. Lett.*, Vol. 70, 147–153, 2017.
15. Shen, Q., W. Liu, W. Cui, and S. Wu, "Extension of co-prime arrays based on the fourth-order difference co-array concept," *IEEE Signal Process. Lett.*, Vol. 23, No. 5, 615–619, 2016.
16. CVX Research Inc., "CVX: Matlab Software for Disciplined Convex Programming, version 2.0 beta," *http://cvxr.com/cvx*, 2013.
17. Grant, M. and S. Boyd, "Graph implementations for nonsmooth convex programs," *Recent Advances in Learning and Control*, V. Blondel, S. Boyd, and H. Kimura (eds.), Springer-Verlag, 95–110, 2008.